

Deformable Liposomal Hydrogel for Dermal and Transdermal Delivery of Meloxicam

This article was published in the following Dove Press journal:
International Journal of Nanomedicine

Zhang Julia Zhang¹
Tomasz Osmałek²
Bożena Michniak-Kohn¹

¹Center for Dermal Research and Ernest Mario School of Pharmacy, Rutgers, The State University of New Jersey, Piscataway, NJ 08854, USA; ²Chair and Department of Pharmaceutical Technology, Poznan University of Medical Sciences, Poznań, 60-780, Poland

Background and Aim: Meloxicam (MX) is a potent hydrophobic non-steroidal anti-inflammatory drug used to reduce inflammation and pain. However, its oral dosage form can cause many adverse gastrointestinal effects. In the present study, a poloxamer P407 based hydrogel system containing transfersomes or flavosomes has been prepared as a potential therapeutic vehicle for the topical delivery of MX.

Methods: In this study, MX was encapsulated in conventional liposomes, transfersomes, and flavosomes. The obtained liposomal vesicles were characterized in terms of size, drug entrapment efficiency, zeta potential, and stability. These MX-loaded liposomal formulations were further incorporated into a poloxamer P407 gel and evaluated using rheological properties, a stability study and an ex vivo permeation study through human cadaver skin by both HPLC analysis and confocal laser scanning microscopy (CLSM).

Results: The developed deformable liposomes exhibited homogeneous vesicle sizes less than 120 nm with a higher entrapment efficiency as compared to conventional liposomes. The deformable liposomal gel formulations showed improved permeability compared to a conventional liposomal gel and a liposome-free gel. The enhancement effect was also clearly visible by CLSM.

Conclusion: These deformable liposomal hydrogel formulations can be a promising alternative to conventional oral delivery of MX by topical administration. Notably, flavosome-loaded gel formulations displayed the highest permeability through the deeper layers of the skin and shortened lag time, indicating a potential faster on-site pain relief and anti-inflammatory effect.

Keywords: flavosome, transfersome, flavonoid, ex vivo skin permeation, poloxamer P407

Introduction

Meloxicam is a Biopharmaceutical Classification System (BCS) class II non-steroidal anti-inflammatory drug (NSAID) structurally related to the enolic acid class of compounds.¹ As a preferential cyclo-oxygenase-2 (COX-2) inhibitor, it has been used clinically to treat osteoarthritis, rheumatoid arthritis, and ankylosing spondylitis by reducing pain and inflammatory symptoms.²⁻⁴ Additionally, it has been widely explored as a potential therapeutic agent for Alzheimer's disease and various tumors, such as lung, colorectal, prostate, and urinary bladder cancers.⁵⁻⁸ However, many adverse effects, especially gastro-intestinal toxicity/bleeding, have been frequently reported when it is administered orally.⁹⁻¹¹ Therefore, topical administration is an appealing alternative because it provides many advantages over the oral route: selective on-site local and systemic effects, avoidance of first pass effect, reduction of gastro-intestinal toxicity, and improvement of patient

Correspondence: Bożena Michniak-Kohn
Center for Dermal Research and Ernest Mario School of Pharmacy, Rutgers, The State University of New Jersey, 145 Bevier Road, Piscataway, NJ 08854, USA
Tel +1 848 445 3589
Fax +1 732 445 5006
Email michniak@pharmacy.rutgers.edu

compliance. As a zwitterionic drug, MX has a relatively high melting point (254°C), low aqueous solubility (7.15 mg/L at 25°C),¹² and lipophilicity (logP=3.43) out of the ideal range of 1–3,¹³ indicating that it is not a suitable candidate for topical delivery.

In order to improve its solubility and lipophilicity, one of the available options is to encapsulate the MX in a liposomal formulation that will improve the solubility and permeability through *Stratum corneum*. In our previous studies, we have used both transfersomes¹⁴ and flavosomes¹⁵ to encapsulate MX and observed improved solubility and skin permeability of MX into the deeper layers of human skin. Transfersomes are considered the first generation of deformable vesicles developed by Cevc and Blume¹⁶ and Cevc et al.,¹⁷ They are generally prepared by addition of a surfactant (edge activator) into the conventional liposomes.¹⁸ Compared to conventional liposomes, the denaturant embedded in the lipid bilayers can destabilize the bilayers and provide a flexible membrane, which enables these vesicles to open extracellular pathways among the cells in the *Stratum corneum*, and then deform to squeeze through these passages into the deeper layers of the skin.^{19–21}

Flavosomes, novel deformable liposomes containing flavonoids, specifically quercetin (QCT) and dihydroquercetin (DHQ), have been developed in our lab. Our study demonstrated that flavonoid-loaded liposomes could be a potential drug delivery system to affect the permeability of encapsulated drugs by modulating the deformability of the liposomal vesicles and fluidity of the *Stratum corneum* membrane.¹⁵

Although suspension dosage forms are easy to apply, the suspended particles are prone to agglomerate, coalesce, and separate, which can lead to non-uniform dosing and instabilities.²² To overcome this, liposomal loaded gel formulation is an appealing alternative dosage form.

Hydrogels are three-dimensional networks consisting of hydrophilic polymers, which have been used for a wide range of applications because of their characteristic properties, such as biocompatibility, biodegradability, and good tolerability.²³ Among these, poloxamer 407 (P407) based hydrogels have been widely studied because of thermoreversible gelation, solubilizing capacity, low toxicity, drug release characteristics, and compatibility with numerous biomolecules and excipients.^{24,25} The most beneficial property of topical formulations based on P407 is reverse thermal gelation of its aqueous solutions. It is the process of viscosity increase upon increasing temperature,

which means that P407-based vehicles bearing liquid-like behavior at lower temperatures become semi-solid as the temperature increases.²⁶ The sol–gel transition point ($T_{\text{sol-gel}}$) strongly depends on composition of the formulation, including concentration of the polymer, active pharmaceutical ingredients, and the additives. This property is considered to be particularly beneficial for skin formulations. By applying a gel with reduced viscosity, it is possible to fill the furrows and crevices in the skin, as well as skin appendages, and thus obtain a larger contact surface, followed by better bioavailability.²⁵

In the present study, a P407 based hydrogel system has been prepared as a potential topical therapeutic vehicle to incorporate MX-loaded liposomal vesicles. A flow diagram is demonstrated in Figure 1.

Materials and Methods

Materials

Phosphatidylcholine (PC) from soybean source was a gift from LIPOID LLC (Newark, NJ, USA). Kolliphor® P407 (P407) was generously donated by BASF Corporation (Tarrytown, NY, USA). Cholesterol (Chol) was purchased from Alfa Aesar (Haverhill, MA, USA). Cetylpyridinium chloride (CPC), quercetin (QCT), ethanol, and isopropanol were purchased from Sigma-Aldrich (St. Louis, MO, USA). Meloxicam (MX) was supplied from Acros Organics (Morris Plains, NJ, USA). Dihydroquercetin (DHQ) was purchased from Cayman Chemical Company (Ann Arbor, MI, USA). High-performance liquid chromatography (HPLC) grade water and acetonitrile were purchased from Sigma-Aldrich and Midland Scientific (Omaha, NE, USA), respectively. 1,1-Dioctadecyl-3,3,3,3-tetramethylindocarbocyanine perchlorate (DiI) was procured from AAT Bioquest (Sunnyvale, CA, USA). Dermatomed human cadaver skin was obtained from New York Firefighter Skin Bank (NY, USA). All other chemicals used were of reagent grade and purchased from VWR International (Radnor, PA, USA).

Methods

Preparation of Liposomes

Meloxicam-loaded liposomes were prepared by the thin film hydration method followed by sonication.^{14,27} The compositions of each formulation are listed in Table 1.

Specific amounts of PC, Chol, CPC, MX, and flavonoids (QCT or DHQ) were first dissolved in chloroform. The lipid mixture was then evaporated under a nitrogen

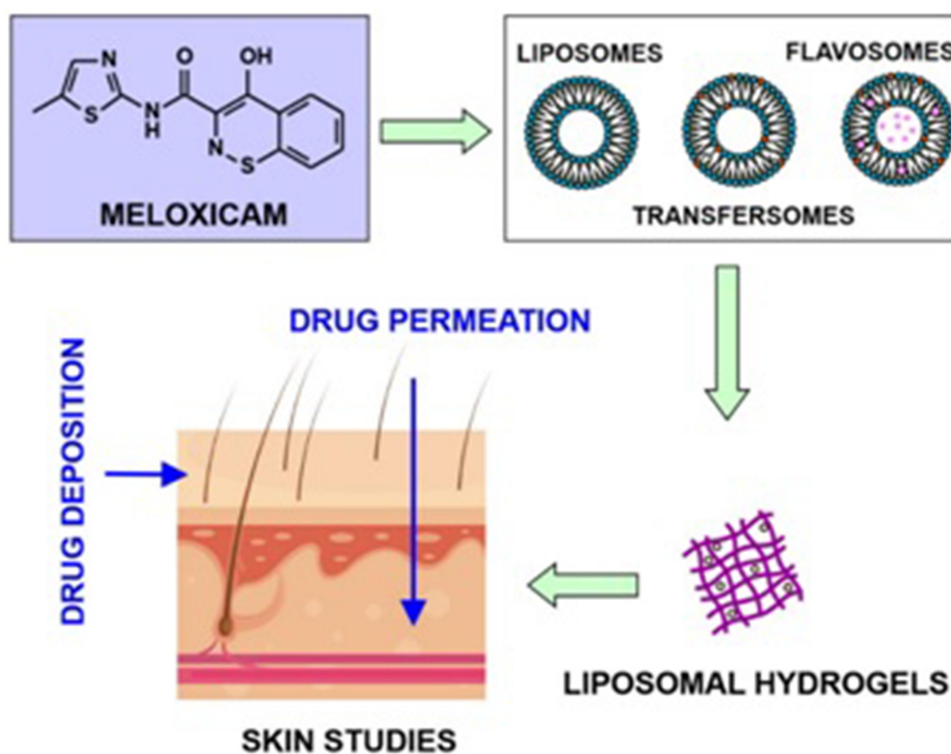


Figure 1 Flow diagram of liposomal hydrogel formulation preparation.

gas stream and the obtained film was placed in a vacuum desiccator overnight to remove any remaining solvent. The dried lipid film was subsequently hydrated with sodium acetate buffer solution (pH 5.5) and sonicated in a sonicator bath (Tru-sweep Crest Bath Ultrasonicator, Cortland, NY, USA) for 1 hour followed by 15 minutes of probe sonication (SFX Branson Ultrasonic Processor, Emerson Industrial Automation, USA) in an ice-water bath. The liposomal suspension was then centrifuged for 30 minutes at 3,000 g. The supernatant was collected in airtight containers and stored under refrigerated conditions prior to use.

HPLC Method of the Quantification of MX

MX was analyzed using high pressure liquid chromatography (HPLC) with UV detection. The HPLC system was an

Agilent 1100 Series liquid chromatograph (Agilent Technologies, Santa Clara, CA, USA) and Agilent Chemstation software (OpenLab CDS, ChemStation Edition, Rev. C.01.10, Agilent Technologies). A reversed-phase C18 column (Agilent Plus C18, 5 μ m, 4.6 \times 150 mm, Agilent Technologies) was used as the stationary phase. The column temperature was maintained at 30.0 \pm 0.2 $^{\circ}$ C. The mobile phase was composed of 1% phosphoric acid (A) and acetonitrile (B) at a flow rate of 1.0 mL/min. The gradient program was: 0 minutes, 32% B; 3.7 minutes, 70% B; 6.7 minutes, 32% B. The UV detector was set at a wavelength of 360 nm for MX. The method was linear at a concentration range 0.05–50 μ g/mL with R^2 of 0.9995 for meloxicam. The limit of detection (LOD) was found to be 0.01 μ g/mL and the limit of quantification (LOQ) was

Table 1 The Composition and Type of the Vesicles Investigated in the Study

Formulation ID	Description	PC ^a (3.2% w/v)	MX ^b (0.32% w/v)	Chol ^c (0.16% w/v)	CPC ^d (0.96% w/v)	QCT ^e (0.24% w/v)	DHQ ^f (0.8% w/v)
CLP	Conventional Liposome	✓	✓	✓			
TFS	Transfersome	✓	✓	✓	✓		
FLSQ	Flavosome Q	✓	✓	✓	✓	✓	
FLSD	Flavosome D	✓	✓	✓	✓		✓

Note: ^aPhosphatidylcholine, ^bMeloxicam, ^cCholesterol, ^dCetylpyridinium chloride, ^eQuercetin, ^fDihydroquercetin.

0.05 µg/mL. The relative standard deviation for both intra-day and inter-day precision was less than 3%.

Measurement of Vesicle Size, Size Distribution, and Zeta Potential

Average size and size distribution (Polydispersity Index, PDI) of the liposome vesicles were measured by Dynamic Light Scattering (DLS) (Zetasizer Nano-S, Malvern Panalytical, USA) with a 632.8 nm He-Ne laser light source (4 mW). Liposomal vesicles were measured as is without any dilution. Then 100 mg of each gel formulation was dispersed in 1 mL of acetate buffer (pH 5.5) using a vortex mixer. Each sample was filled in a disposable polystyrene low volume cuvette (ZEN0118) without further treatment, and equilibrated prior to the experiment for 180 seconds. The measurements were done at 25.0°C using non-invasive backscatter mode (NIBS) at an angle of 173°.

Zeta potential was determined by Electrophoretic Light Scattering (ELS) (Zetasizer Nano series, Malvern Panalytical, USA). All formulation samples without further treatment were filled in disposable capillary zeta cells (DTS1070) and analyzed at 25°C.

Determination of MX Entrapment Efficiency and Drug Loading

The prepared liposomal vesicles were disrupted with 50% v/v ethanol in water and sonicated for 10 minutes in a sonicator bath (Tru-sweep Crest Bath Ultrasonicator, Cortland, NY). The resulting solution was then filtered with a 0.45 µm nylon syringe filter (Midland Scientific, Omaha, NE) and the concentrations of MX in the vesicle formulation were determined using HPLC analysis. The entrapment efficiency of MX loaded in the liposomes was calculated as per Equation (1),²⁸ whereas the drug loading (drug-to-lipid ratio) was calculated as per Equation (2):²⁹

$$\% \text{ entrapment efficiency} = (C_M/C_i) \times 100 \quad (1)$$

$$\% \text{ drug loading} = (C_M/C_L) \times 100 \quad (2)$$

where C_M is the concentration of MX loaded in the liposome, as described in the above methods, C_i is the initial concentration of MX added into the vesicle formulation, and C_L is the concentration of phosphate lipid added into the vesicle formulation.

Degree of Deformability

The vesicles were passed through a 50 nm polycarbonate membrane (GE Healthcare, Chicago, IL, USA) fitted on an

extruder (Avanti Polar Lipids, Alabaster, AL, USA). Vesicles before and after extrusion were analyzed for vesicle size and deformability index. Vesicle size was analyzed following the procedure described in Measurement of Vesicle Size. The deformability index was calculated by dividing vesicle size before and after extrusion.³⁰

Preparation of Liposomal Gel

Liposomal gel was prepared using P407 by “cold method” as described by Dumortier et al.²⁵ Specified amounts of P407 (20% w/w) and liposomal formulations were mixed in an ice-water bath with continuous magnetic stirring, until a homogeneous dispersion was obtained. Concurrently, a specific amount of P407 (20% w/w) dispersed in MX saturated PBS (pH 7.4) was prepared as the plain (liposome-free) gel formulation. The mixture was then kept overnight at 4°C to ensure complete dissolution of P407. Subsequently, the dispersion was gently mixed at room temperature until a consistent gel formed.

Morphology of Liposomal Vesicles and Gel Formulations

The morphology of liposomal vesicles and gel formulations was characterized by transmission electron microscopy (TEM) (CM 12 TEM, Philips, Amsterdam, Netherlands). Then 100 mg of each gel formulation was dispersed in 1 mL of acetate buffer (pH 5.5) using a vortex mixer. One drop of liposomal vesicle or prepared gel formulation solution was placed onto a copper grid and the excess solution was immediately adsorbed using filter paper. The sample was then stained by adding a drop of 2% phosphotungstic acid. The excess solution was immediately removed by filter paper, and then the sample was dried at room temperature. Afterward, the grid was observed using a TEM with AMT Image Capture Engine V602 (Advance, Microscopy Techniques Corp, Woburn, MA, USA).

Oscillatory Rheology Studies

The oscillatory rheological measurements were performed on Kinexus Ultra+ (Malvern Pananalytical Ltd., USA) rotational rheometer with rSpace software (ver. 1.75.2326, Malvern Pananalytical Ltd., USA). The samples were tested with the use of stainless-steel plate-plate geometry ($\Phi=20$ mm). The measuring gap was set at 1.0 mm. Prior to the experiments, the samples were placed on the lower plate. After lowering down of the upper plate, the excess was removed with a spatula. Each measurement

was conducted in triplicate using fresh samples, and the mean values of the parameters were reported.

The measurements, including oscillatory stress sweeping (SS) and temperature sweeping (TS), were performed sequentially in a single run. After being placed in the rheometer, the samples were equilibrated for 2 minutes at $32.0 \pm 0.5^\circ\text{C}$. Then the SS study was performed in the range of 1.0–12,000.0 Pa. In the second step, the samples were cooled to $5.0 \pm 0.5^\circ\text{C}$ and a TS ramp was conducted in the range of 5.0 – 30.0°C , at constant stress of 2.0 Pa. For both SS and TS measurements, the oscillation frequency was set at 1.0 Hz.

The results for SS studies were presented as the dependence of storage (G') and loss (G'') moduli vs oscillatory stress (τ), plotted in a logarithmic scale. Additionally, the G'/G'' cross-over points were calculated. Temperature sweeping results were plotted as G' dependence on temperature.

Ex vivo Skin Permeation Study

Full thickness dermatomed (approximately 500 μm) human cadaver skin from the posterior torso was obtained from the New York Firefighters Skin Bank (New York, NY, USA). On the day of study, the skin was quickly thawed in pH 7.4 PBS at room temperature for 20 minutes. An appropriate size of skin was cut using a pair of scissors and carefully mounted on the receptor chamber of a vertical Franz Diffusion Cell (FDC) (Logan Instruments, Somerset, NJ, USA) filled with a known volume of pH 7.4 PBS buffer and an orifice size of 0.64 cm^2 , the *Stratum corneum* facing the donor chamber. The FDC was then placed into a dry block heater (Logan Instruments) set at $37.0 \pm 0.5^\circ\text{C}$, and was stirred continuously with a small PTFE-coated magnetic bar at 600 rpm.

After the assembled FDC was equilibrated for at least 30 minutes, approximately 500 mg of each MX loaded liposomal gel formulations and liposome-free gel formulation was applied to the skin. At appropriate time intervals, an aliquot of the receptor medium was withdrawn, and the same volume of fresh buffer solution was replaced to the receptor chamber. The concentration of MX in the aliquot was analyzed using the HPLC method described above.

At the end of the permeation study (24 hours), the donor compartment was removed. The skin sample was washed with PBS buffer (pH 7.4) to remove the residual formulations and carefully dried with a cotton swab. Next, the section of skin exposed to the test formulation was cut out with scissors and the dermal and epidermal layers were separated manually with tweezers. Separated layers were

cut into small pieces and collected into a beadbug prefilled tube. Then the obtained samples were homogenized with 1 mL of 50% ethanol using a BeadBug Microtube Homogenizer (Model D1030, Benchmark Scientific Inc., Sayreville, NJ, USA) for three cycles of 3 minutes (total 9 minutes). The resulting solutions were centrifuged at 10,000 rpm for 5 minutes (Eppendorf Centrifuge 5415c, Brinkmann Instruments, Inc., Westbury, NY, USA). The supernatant was then filtered and collected into an HPLC vial using $0.45\text{ }\mu\text{m}$ syringe filters. Collected samples were analyzed using the HPLC method described above.

The cumulative amount of MX permeated per unit area was calculated according to Equation (3):³¹

$$Q_n = \frac{C_n V_r + \sum_{i=0}^{n-1} C_i V_s}{A} \quad (3)$$

where Q_n is the cumulative amount of the drug permeated per unit area ($\mu\text{g}/\text{cm}^2$) at different sampling times, C_n is the drug concentration in the receiving medium at different sampling times ($\mu\text{g}/\text{mL}$), C_i is the drug concentration in the receiving medium at the i th ($n-1$) sampling time ($\mu\text{g}/\text{mL}$), V_r is the volume of the receptor solution (mL), V_s is the volume of the sample withdrawn (mL), and A is the effective permeation area of the diffusion cell (cm^2). The Q_n values were plotted against time, and then the steady-state flux (J_{ss}) was calculated from the slope of the linear portion of the plot.

The permeability coefficient (K_p) was calculated with Equation (4):³²

$$K_p = \frac{J_{ss}}{C_0} \quad (4)$$

where C_0 represents the initial concentration of MX in the donor compartment.

Fluorescence Microscopy

The depth of the skin penetration of the liposomal gel was evaluated by fluorescence microscopy (LSM 780 Confocal Laser Scanning Microscope; Zeiss Research Microscopy Solutions, Pleasanton, USA). Dil dye was prepared and added in the lipid–drug–chloroform solution (at a 1:50 ratio, w/w) before the drying process. Dil-loaded liposomal formulations were then prepared as the procedure described in Preparation of Liposomes. Subsequently, these Dil-labeled vesicles were incorporated in 20% (w/w) P407 gel formulations prepared using the procedure described in the Preparation of Liposomal Gel section. Permeation studies of these liposomal gel formulations were then performed under the same conditions as described in the Ex Vivo Skin

Permeation Study. After application for 24 hours, the residual amount of the gel formulations was removed from the donor compartment. The skin exposed to the formulation was washed with deionized water and then dried with a cotton swab. Subsequently, the skin sample was mounted on a microscope slide. The specimen was optically scanned at 10 μm increments without any additional staining or treatment through a 10 \times objective using a fluorescence microscope equipped with a filter for Dil dye. The images were then analyzed using ImageJ 1.52p software (NIH, USA).

Effect of Storage

The effect of storage study for liposomal suspensions and liposomal gel formulations was conducted at 5 \pm 3 $^{\circ}\text{C}$ and 25 \pm 5 $^{\circ}\text{C}$, respectively, for a period of 90 days. The content of MX contained in these vesicles and gel formulations were evaluated by the HPLC method described above at intervals of 30, 60, and 90 days.

Statistical Analysis

The data were reported as means \pm SD (n=3). The obtained results were analyzed with one-way analysis of variance (ANOVA) followed with post-hoc Tukey's test. Statistical significance in the differences of the means was determined by Student's *t*-test. The statistical significance level in all tests was set at 5%. All calculations were performed with JMP[®] Pro 14.2.0 (SAS Institute Inc., Cary, NC, USA).

Results and Discussion

Characterization of MX-Loaded Liposomes

The formulations developed in the previous studies^{14,15} had low MX content, so the resulting gel formulations did not yield any meaningful permeation results. Therefore, we modified the liposomal formulations as summarized in Table 1 in the present study to increase the content of MX. As demonstrated in many published studies,^{33–35} the composition of the liposome systems

determines their efficacy by affecting the size, size distribution, zeta potential, drug content, and entrapment efficiency of the vesicle formulations. For example, many studies revealed that cholesterol has a significant effect on the physicochemical properties of liposomes. However, numerous studies have reported contradictory effects of cholesterol on size, zeta potential, and drug entrapment. For example, Tavano et al³³ reported the incorporation of cholesterol decreased the size of liposomes. On the contrary, the study of Lopez-Pinto et al³⁶ revealed the increase of liposomal size with the incorporation of cholesterol. However, as our study¹⁴ revealed, the addition of cholesterol did not have much effect on the physicochemical properties of the investigated liposomal vesicles. As the size, vesicle surface charge, and amount of encapsulated drugs of the vesicles can affect their permeability, it is important to characterize the prepared MX-loaded liposomes with respect to their particle size, polydispersity index (PDI), zeta potential, and %EE (Table 2).

The entrapment rates of MX in the vesicles were in the range of approximately 0.3–3 mg/mL. The solubility of MX in acetate buffer solution (pH 5.5) was determined to be 6.82 \pm 0.30 $\mu\text{g/mL}$ (n=3), indicating that liposomal formulations provided substantial enhancement of MX solubility. It was observed that %EE for MX was significantly higher in deformable liposomes compared to those in conventional liposomes. These results might be attributed to the intrinsic properties of the cationic surfactant, CPC, as a solubilizer and the interactions among the surfactants, MX, and lipid bilayer. The presence of embedded edge activator (surfactant), CPC, can help solubilize MX in the liposomal lipid bilayer, which could significantly increase the %EE of the encapsulated drugs. This observation is in agreement with the data obtained by Duangjit et al.^{28,37} The authors state that cationic surfactants act as solubilizers for the drug in the liposomal bilayer. Moreover, they

Table 2 Physicochemical Properties of the Obtained Vesicles. Data are Presented as Means \pm SD (n=3)

Sample ID	Description	MX ^a			Average Diameter (nm)	PDI ^d	Zeta Potential (mV)
		%EE ^b	%DL ^c	Content (mg/mL)			
CLP	Conventional Liposome	9.13 \pm 1.13	0.91 \pm 0.11	0.292 \pm 0.036	111.4 \pm 0.2	0.257 \pm 0.008	2.1 \pm 0.3
TFS	Transfersome	96.04 \pm 1.98	9.61 \pm 0.20	3.075 \pm 0.063	62.3 \pm 0.3	0.287 \pm 0.013	32.2 \pm 0.6
FLSQ	Flavosome-Q	94.39 \pm 1.57	9.44 \pm 0.16	3.022 \pm 0.050	66.0 \pm 0.6	0.281 \pm 0.002	27.8 \pm 0.5
FLSD	Flavosome-D	92.24 \pm 0.36	9.23 \pm 0.04	2.954 \pm 0.011	97.0 \pm 1.3	0.298 \pm 0.023	23.6 \pm 0.7

Note: ^aMeloxicam, ^bEntrapment Efficiency, ^c%Drug Loading, ^dPolydispersity Index.

can affect the net positive charge of the bilayer, destabilize it, and increase the elasticity of the vesicles. A similar effect has also been observed in the case of ethosomes. As Marto et al²⁰ disclosed in their study, incorporating ethanol into the liposomal formulation can solubilize the drug and create deformable lipid structures which could easily pass between skin corneocytes and subsequently enhance the skin retention and permeation.

The isoelectric point (pI) of MX was reported to be 2.6,²⁸ which is lower than the pH of hydration buffer (pH 5.5). Therefore, MX is presented in negatively charged form in our developed formulations. As was mentioned above, CPC is a cationic surfactant which may contribute to the increased entrapment efficiency as a result of attractive electrostatic interactions between the negatively charged drug molecules and the surfactant.

The %EE of MX in transfersome was 96.04%, which was higher than the values obtained for QCT/DHQ loaded flavosomes (94.39% and 92.24%, respectively). The observed effect may be due to the fact that the flavonoids could compete with MX to reside in the vesicle bilayers. Furthermore, the diameter of the transfersome vesicles was significantly lower than these two flavosomes types, which may also be an indication that the effect described above does happen. Moreover, higher %EE correlated with lower vesicle diameter observed for transfersomes have also been reported by other authors.^{38,39}

The vesicle sizes of all these liposomal formulations were in the nano-size range of 60–110 nm, with the size distribution (polydispersity index; PDI) of 0.2–0.3. Deformable liposomes had smaller vesicle sizes compared to conventional liposomes, due to the incorporation of edge activator, CPC, which can achieve higher curvature, thus resulting in a decrease in vesicle size compared to conventional liposomes. The particle size in flavosomes was higher than that in transfersomes, probably because more components had been encapsulated in these liposomes, which is in agreement with our prior study.¹⁵

Zeta potential was used to quantitate the surface charge of these vesicles. The zeta potentials of these vesicles were in the positive range of 2–32 mV (Table 2). The results ranked in order of positive charge as transfersomes>flavosome-Q>flavosome-D>>conventional liposomes. The observed differences indicate that deformable liposomes reveal a higher tendency to resist aggregation and therefore provide better stability.

As disclosed by Cevc and Blume¹⁶ and Hua⁴⁰, the embedded edge activator can destabilize the deformable

liposomal lipid bilayers and enable these vesicles to penetrate through extracellular pathways among the skin cells within the *stratum corneum*. Then these flexible vesicles could deform to squeeze into the deeper layers of the skin. Therefore, deformability is one of the important characteristics of these flexible vesicles to measure their ability to squeeze through pores smaller than the liposomal diameters. The degree of deformability of each liposomal formulation were determined and are summarized in Table 3.

The deformability index of conventional liposomes was found to be around 50 nm, which coincided with the size of the polycarbonate membranes (50 nm) used, indicating that the vesicles were quite rigid. However, the deformability indices of deformable liposomes, ie, transfersomes and flavosomes, were much greater than those of conventional liposomes. This suggested that the deformable vesicles regained their size after extrusion. It is noteworthy that the deformability indices of flavosomes were found to be close to 1, indicating that incorporating DHQ and QCT into the liposomes could affect the elasticity of vesicles by changing the fluidity and stability of the lipid bilayer.

To further characterize these vesicle systems, a TEM study was conducted for these developed liposomal vesicles. Figure 2A–D presents the TEM images for CLP, TFS, FLSQ, and FLSD, respectively, which show spherical shapes for all these vesicle formulations.

Characterization of MX-Loaded Hydrogels

Gels are transparent semisolid emulsions which contain a gelling agent to provide stiffness to a solution or colloidal dispersion (suspension) for external application to the skin.⁴¹ This dosage form provides many advantages over

Table 3 Deformability Index of Liposomal Vesicles. Data are Presented as Means±SD (n=3)

Formulation	Particles Size Before Extrusion (nm)	Particles Size After Extrusion (nm)	Deformability Index
CLP	105.2±0.7	59.0±0.4	0.561±0.004
TFS	80.8±0.6	67.6±1.0	0.837±0.012*
FLSQ	82.4±0.7	79.8±0.7	0.969±0.008*
FLSD	96.1±1.4	95.8±0.1	0.997±0.001*

Note: *P<0.05 vs CLP.

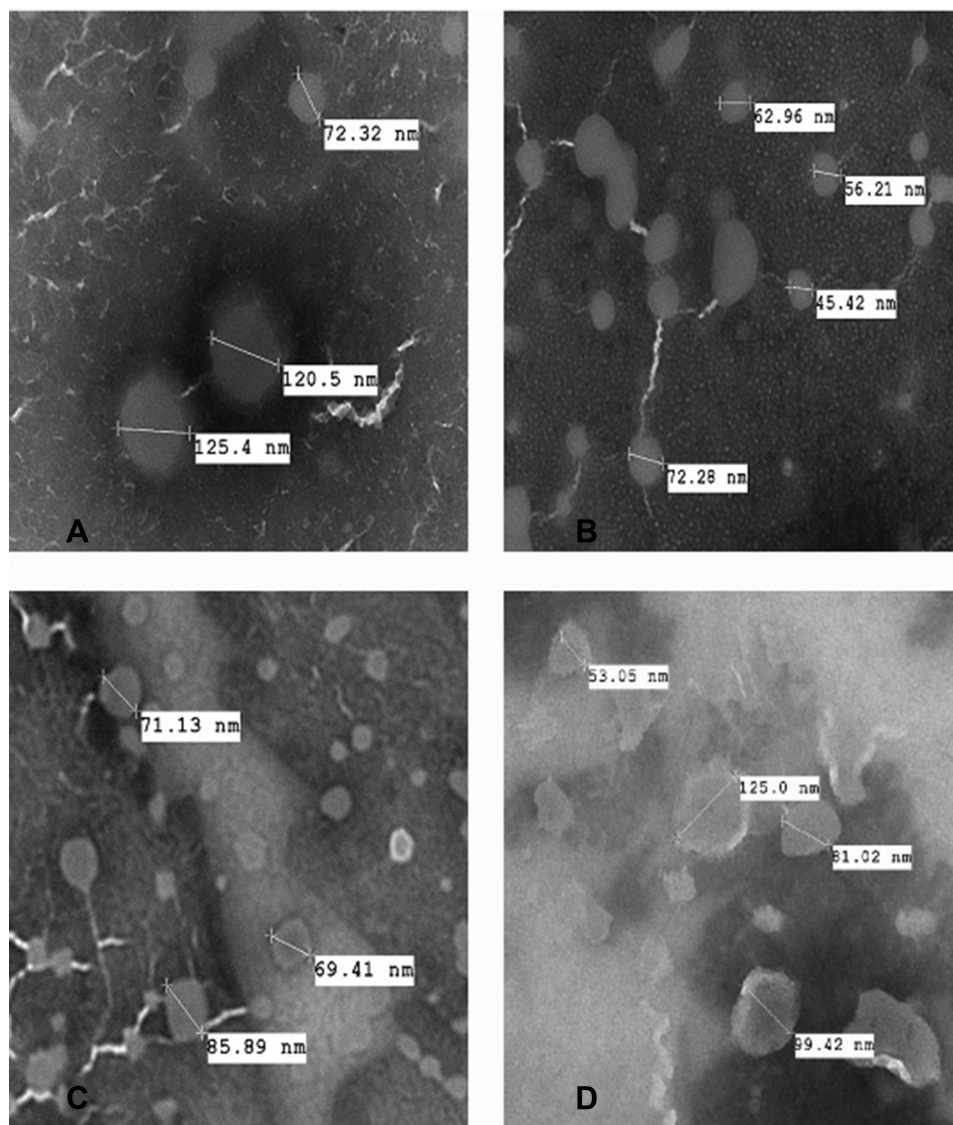


Figure 2 Transmission electron microscopy images of (A) conventional liposomes; (B) transfersomes; (C) flavosomes-Q; (D) flavosomes-D.

suspensions, because it has less long-term stability issues, good adherence property to the site of application, and better patient compliance. Furthermore, it can be used as a controlled release formulation.⁴²

Assessment of the mechanical properties is one of the crucial stages in the development of semi-solid formulations. For this purpose, multiple techniques are used, including tension/compression analysis, dynamic mechanical analysis (DMA), and oscillatory rheology. The latter one is a very precise tool that provides data on the viscoelastic properties. Viscoelasticity describes materials that can behave both like elastic solids and viscous fluids. Viscoelastic properties correlate with the physical appearance of semi-solid drug delivery systems, influence

patient's perception, but also affect the therapeutic efficiency.^{43,44}

The oscillatory stress sweeping (SS) was performed to monitor the values of storage (G') and loss moduli (G'') upon increasing oscillatory stress. The angular frequency of the oscillation was constant during the experiments (1.0 Hz=6.2832 rad/s). To analyze the effects of drug and carriers on the polymer network stability, the measurements were conducted for all liposomal gels and compared to the properties of a blank liposomal gel (BLK-Gel) without actives (MX/QCT/DHQ) and a gel containing the drug in a dissolved form, without liposomes (MX-Gel). The logarithmic plots presented in Figure 3A showed that all gels revealed a wide range of linear viscoelasticity, termed

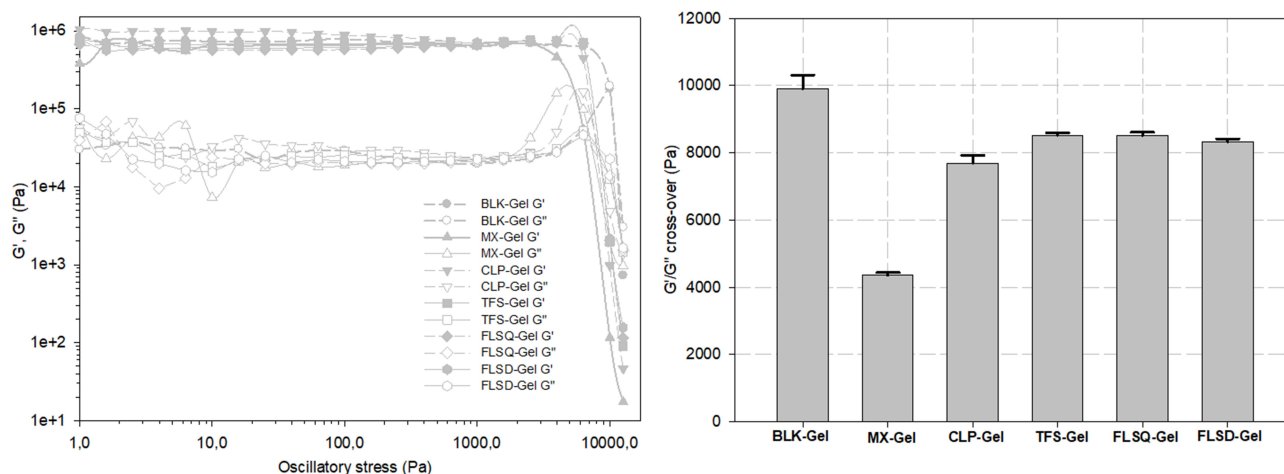


Figure 3 Amplitude sweeping plots obtained for the gels (A) and calculated cross-over values (B) ($n=3$ for each formulation, data are presented as means \pm SD).

LVR (Linear Viscoelastic Region), where the values of storage modulus (G') remained constant and independent of the increasing stress. As observed, the values of G' in LVR were predominantly higher than those of G'' , which clearly indicates that the tested gels were more elastic than fluid-like. The LVR was also determined to depict the stability of the gels structure, since structural properties are best related to elasticity. Samples with broad LVR can be classified as well-dispersed and stable.

Also demonstrated in Figure 3A, the values of both moduli became less distinct above LVR, which can be attributed to maximum extension of the polymer chains and partial breakage of hydrogen bonds. From the SS plots, the cross-over points were determined and graphed in Figure 3B. This parameter is the value of stress at which the moduli equalize and depicts the moment of entire gel structure breakage. As revealed in Figure 3B, the BLK-Gel was the most durable, while the MX-Gel turned out to be most prone to deformation, which was depicted by lower value of cross-over point, of approximately 55%. The mechanical stability of MX-loaded liposomal gel formulations decreased about 20% in comparison to BLK-Gel. It can be stated that addition of MX decreased the gel durability, most probably by weakening the interactions between hydrophobic polypropylene oxide (PPO) chains. In the case of MX loaded liposomal gels, the effect was less significant because of partial incorporation of the drug, however the observed effect could also be related to adherence of PPO blocks to the surface of liposomes or partial embedding into the phospholipid layer.⁴⁵

Oscillatory measurements were also performed to determine the thermal transition of the gels. Samples

were subjected to increasing temperature in the range of 5.0–40°C and the G' value was monitored. As presented in Figure 4, none of the gels revealed a sharp transition from liquid to semi-solid form ($T_{\text{sol-gel}}$). In all cases the structure was forming in a wide temperature range. The highest $T_{\text{sol-gel}}$ was observed for MX-Gel which was correlated with the data obtained in the previous experiment. This confirmed that the weaker the structure, the higher the gelation temperature. The BLK-Gel started to thicken at the lowest temperature (~ 6 –7°C). Similar behavior was observed for the MX-loaded deformable liposomal gels, while a conventional liposomal gel formulation recorded similar $T_{\text{sol-gel}}$ as that of MX-Gel, indicating it was less stable than the deformable liposomal gel formulations.

To study the morphology of these prepared gel formulations, a TEM analysis was performed. Figure 5A–E present the obtained TEM images for MX-Gel, CLP-Gel, TFS-gel, FLSQ-Gel, and FLS-D gel, respectively. Stained spherical shape vesicles were observed in liposomal gel formulations, but it was absent in MX-loaded plain Poloxamer P407 gel, as expected.

The apparent particle size and size distribution were also determined for these liposomal gel formulations and the data obtained was compared with those of the liposomal vesicles and summarized in Table 4. It suggested that the particle size increased with the addition of poloxamer P407. A similar observation was also disclosed in the study conducted by Pandita et al.⁴⁶ In the study, they suggested that the increased viscosity of the outer phase caused by the increase of poloxamer concentration might be the reason of the particle size increase. As stated in the technical note provided by Malvern Instrument,⁴⁷ the particle size determination using

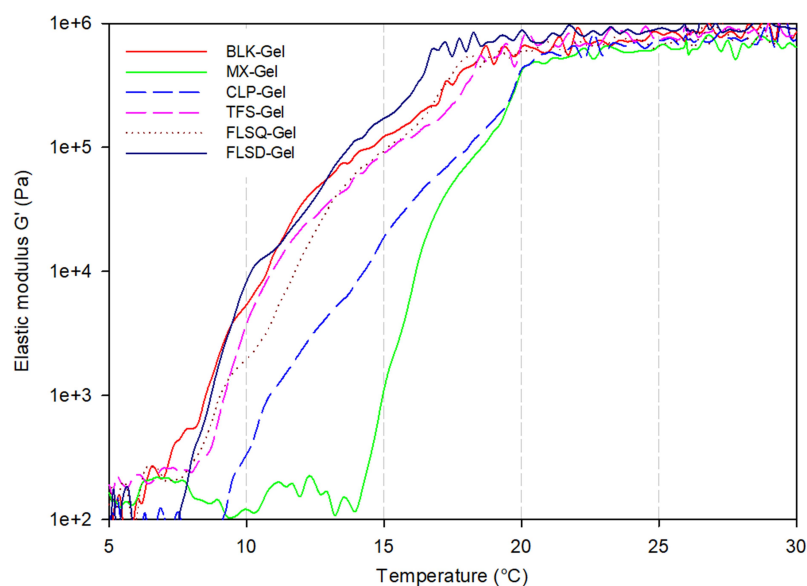


Figure 4 Temperature sweeping of the gels ($n=3$ for each formulation, data are presented as means \pm SD).

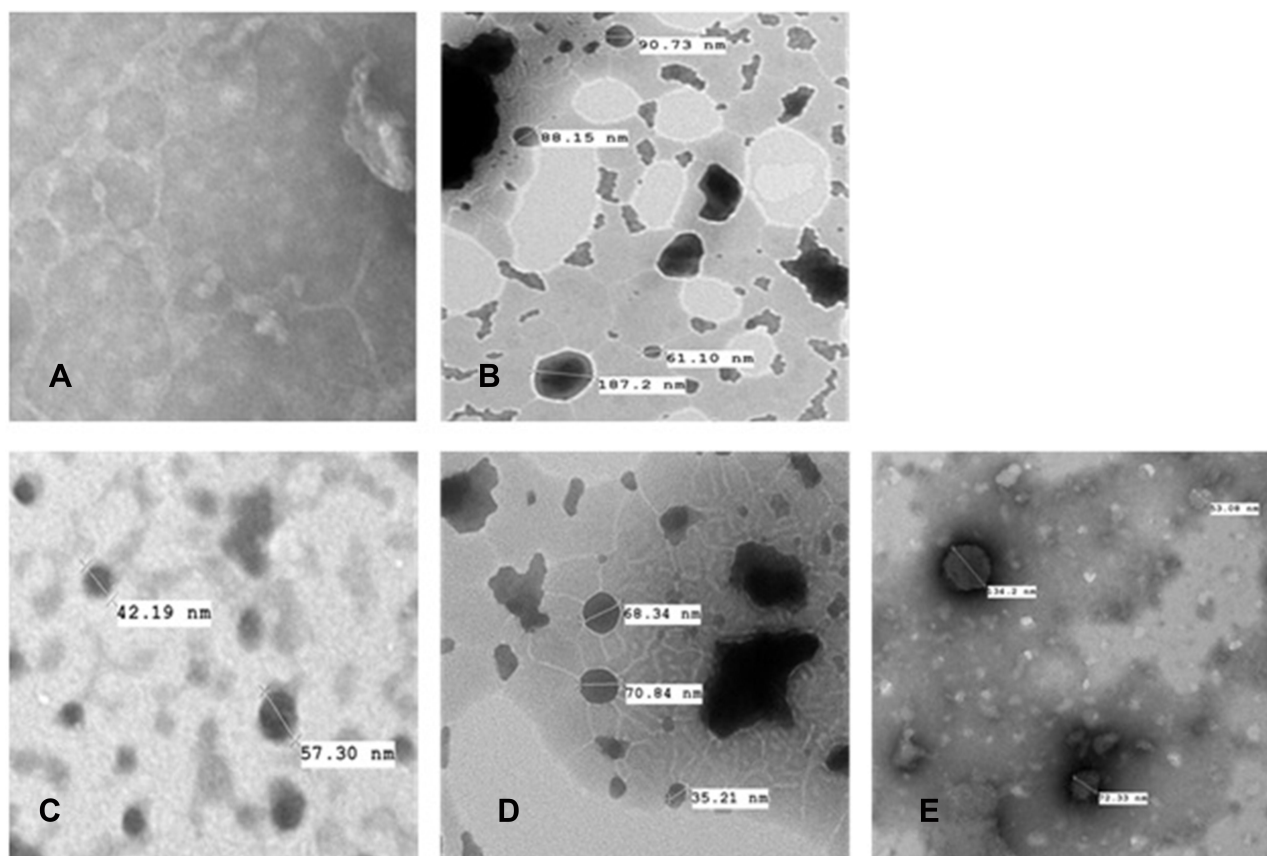


Figure 5 Transmission electron microscopy images of (A) MX-gel, (B) CLP-gel, (C) TFS-gel, (D) FLSQ-gel, (E) FLSD-gel.

Dynamic Light Scattering technique can be affected by the ionic strength of medium, surface structure, viscosity, and non-spherical particles. Therefore, the apparent particle size observed in these gel formulations might not directly

describe the particle size of the embedded vesicles. This is supported by the TEM images shown in Figure 5, in which the liposomal vesicles embedded in the hydrogel had a similar particle size with those in the suspensions.

Table 4 Physical Properties of the Obtained Liposomal Vesicles and Liposomal Gel Formulations. Data are Presented as Means \pm SD (n=3)

Sample ID	Description	Liposomal Vesicles		Liposomal Gel	
		Average Diameter (nm)	PDI ^a	Average Diameter (nm)	PDI
CLP	Conventional Liposome	111.4 \pm 0.2	0.257 \pm 0.008	245.4 \pm 3.4	0.133 \pm 0.012
TFS	Transfersome	62.3 \pm 0.3	0.287 \pm 0.013	231.0 \pm 1.2	0.147 \pm 0.015
FLSQ	Flavosome-Q	66.0 \pm 0.6	0.281 \pm 0.002	236.2 \pm 1.8	0.187 \pm 0.015
FLSD	Flavosome-D	97.0 \pm 1.3	0.298 \pm 0.023	246.8 \pm 5.2	0.178 \pm 0.023

Note: ^aPolydispersity Index.

Table 5 Permeation Parameter Obtained for the Investigated Gel Formulations. Data are Presented as Means \pm SD (n=3 for Each Formulation)

Formulation	J _{ss} ^a (μ g/cm ² /h)	Concentration (μ g/mg) ^c	K _p ^b (mg/cm ² /h)	Enhancement Ratio	Lag Time (h)
CLP-gel	–	0.219 \pm 0.005	–	–	–
MX-gel	0.017 \pm 0.006	0.428 \pm 0.057	(3.93 \pm 1.47) $\times 10^{-2}$	1	4.17 \pm 1.34
TFS-gel	0.128 \pm 0.010*	1.906 \pm 0.014	(6.71 \pm 0.52) $\times 10^{-2}$ *	1.71	4.42 \pm 0.60
FLSQ-gel	0.222 \pm 0.014* [#]	1.885 \pm 0.030	(11.78 \pm 0.76) $\times 10^{-2}$ * [#]	3.00	2.54 \pm 0.77 [#]
FLSD-gel	0.245 \pm 0.010* [#]	2.064 \pm 0.042	(11.89 \pm 0.50) $\times 10^{-2}$ * [#]	3.03	2.89 \pm 0.55 [#]

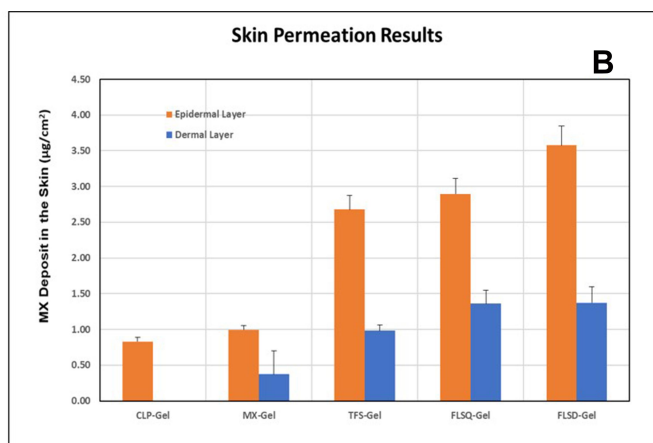
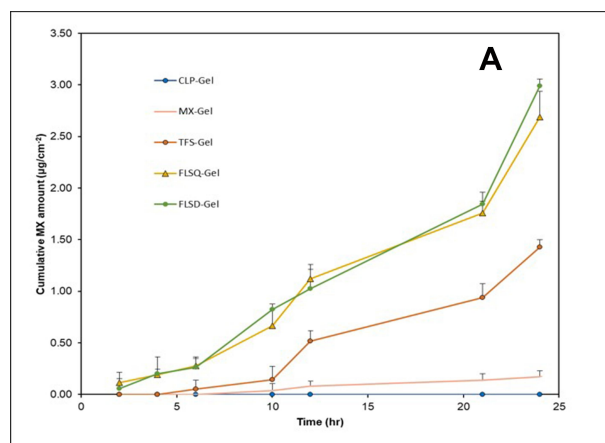
Note: *P<0.05 vs MX-gel, [#]P<0.05 vs TFS-gel, ^aJ_{ss}: steady-state flux, ^bK_p: permeability coefficient, ^cConcentration is expressed as μ g of meloxicam/mg of gel formulation.

Ex vivo Skin Permeation Study

To study the potential of topical delivery of MX using these liposomal hydrogel prototypes, the ex vivo skin permeation study through human cadaver skin was conducted using Franz diffusion cells. The content of MX in the liposomal gel was targeted at 2 mg/g with the exception of CLP-gel due to its low entrapment efficiency. A gel formulation with MX dissolved in pH 7.4 PBS (MX-Gel) was also prepared as control. The concentration of MX in each formulation is summarized in Table 5. The drug permeation profiles of MX plotted as a function of time and amount of MX deposited in

the epidermal and dermal layers after skin permeation study are shown in Figure 6A and B, respectively. The values of steady state fluxes (J_{ss}), permeability coefficients (K_p), enhancement ratio, lag time, and correlation coefficient (r²) are presented in Table 5.

As demonstrated in Figure 6, compared to MX-gel, no MX content was observed in donor compartments and the dermis when the CLP-gel formulation was applied, despite that a similar level of MX was obtained in the epidermis. This may indicate that the rigid structure of conventional liposomes prevented their transport to the deeper layer of

**Figure 6** (A) Ex vivo drug permeation profiles of meloxicam (MX)-loaded liposomal gel formulations over 24 hours; (B) MX deposited in the different layers of skin after 24-hour skin permeation study from formulations tested (n= for each formulation, data are presented as means \pm SD).

the skin. Therefore, it revealed that conventional liposomal gel did not produce any benefit over a simple MX gel formulation.

However, deformable liposomal gel formulations, TFS-gel, FLSQ-gel, and FLSD-gel, recorded a higher amount of MX observed in the receptor compartments and distributed in the different layers of skin, compared to the controls, CLP-gel and MX-gel. Moreover, the highest MX content was obtained when flavosome loaded gel formulations were applied on the skin.

To discount the effect of different MX concentrations, K_p of these investigated formulations was determined and recorded in Table 5. Subsequently, the enhancement ratios were calculated by dividing K_p of each deformable liposomal gel formulation against K_p of MX-gel. The enhancement ratios of TFS-gel, FLSQ-gel, and FLSD-gel were found to be 1.71, 3.00, and 3.03, respectively, indicating flavosomal loaded gel formulations showed the highest permeation. Additionally, the lag time for flavosomal gel formulations are shorter than those found for TFS-gel and MX-gel, revealing a faster on-site release of MX by these two formulations. This indicated a potential benefit for faster pain relief and anti-inflammatory effect by utilization of the flavosomal drug delivery system.

The obtained results are in good agreement with numerous studies which confirm that classical liposomes have limited value of promoting skin delivery of various drugs due to the fact of insufficient skin penetration ability, which is the result of low deformability.⁴⁸ As it was proven, intact liposomes are not able to penetrate into the granular layers of the epidermis.⁴⁹ The positive effect of flavonoids on skin penetration of MX can be the result of two mechanisms. First, it can be attributed to their influence on the deformability of the vesicles followed by deeper penetration into the skin. Second, by interaction with *stratum corneum*, flavonoids can increase the fluidity of lipid layers and therefore promote translocation of the drug. Numerous studies confirmed that QCT and DHQ reveal a high ability to interact with the lipid bilayers and increase the fluidity of phosphatidylcholine liposome membranes.^{50–52} The interaction is described as strongly concentration- and pH-dependent.^{53,54} The changes in physical properties of the lipid bilayers are the result of interstitial embedding into the hydrophobic domains or the polar headgroup domains. Such behavior may be related to both the lipophilic nature of QCT/DHQ and their interactions with the polar headgroups of phospholipids.

Table 6 Kinetic Models for the Investigated Gel Formulations

Formulation	Zero Order		First Order		Higuchi Model	
	K ^a	r ² b	K	r ²	K	r ²
MX-Gel	0.008	0.969	0.04	0.873	0.053	0.919
TFS-Gel	0.064	0.936	0.074	0.873	0.399	0.861
FLSQ-Gel	0.111	0.955	0.059	0.924	0.701	0.898
FLSD-Gel	0.123	0.947	0.067	0.867	0.774	0.889

Note: ^aK: slope, ^br²: correlation coefficient.

The release kinetics of these liposomal gel formulations was calculated using zero order, first order, and Higuchi model, and the obtained results are summarized in Table 6. The best fit with the highest correlation coefficient (r^2) was found to be zero-order for all formulations. Therefore, J_{ss} was determined over the period of 0–24 hours with the correlation coefficient (r^2) for these formulations ranging from 0.94–0.97, displaying a zero-order release profile.

Moreover, the release profiles of TFS-gel and FLS-gel displayed a two-phase release, as demonstrated in Figure 6A. The permeation rate accelerated after 10 hours for TFS-gel and 6 hours for FLS-gel, respectively. As illustrated in detail by El Maghraby et al,¹⁹ the transdermal delivery mechanisms of liposomal systems can be categorized into: a) free drug, b) penetration enhancing, c) vesicle adsorption to and/or fusion with the SC, d) intact vesicular skin penetration, and e) transappendageal penetration.

The main potential delivery routes could be b), c), and d) for these deformable liposomes under these testing conditions. However, the efficiency and the extent of each route contributing to the delivery of MX into the receptor compartment may be very different. Therefore, for Phase 1, the passive diffusion of MX might be driven by one or two of these delivery mechanisms, while all three delivery routes contribute to accelerate the permeation rate in Phase 2.

Skin Penetration of Dil-Labeled Liposomal Gel Formulations

The depth of the full thickness human cadaver skin penetration of the Dil-labeled vesicles containing gel formulations was evaluated using fluorescence microscopy. According to the Confocal Laser Scanning Microscopy (CLSM) images displayed in Figure 7, CLP-gel, TFS-gel, FLSQ-gel, and FLSD-gel penetrated into the skin up to 30, 120, 180 and 210 μm , respectively.

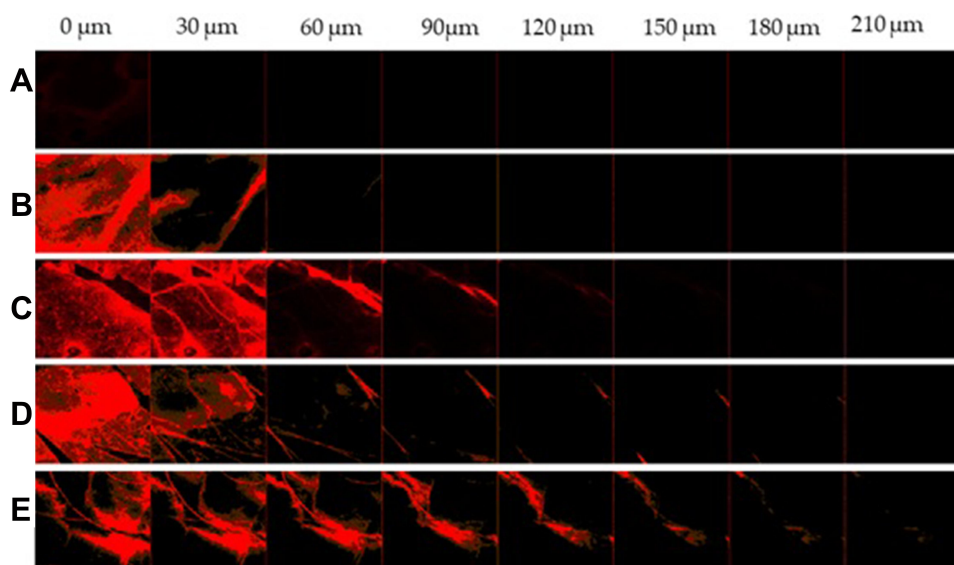


Figure 7 Confocal laser scanning microscopy images taken at different depths of the full thickness human cadaver skin after 24 hours permeation of DiI-labeled gel formulations containing (A) untreated skin, (B) CLP-gel, (C) TFS-gel, (D) FLSQ-gel, and (E) FLSQ-gel (magnification 10X).

The observed results indicated gel formulations containing deformable liposomes had higher skin permeability than conventional liposomes. Among the deformable liposomal formulations, flavosomal gel formulations displayed the highest permeability through the deeper layers of the skin. These findings confirmed the observations described above.

Effect of Storage Study for Liposomal Formulation and Gel Formulation

The effect of storage study has been conducted on liposomal suspensions and gel formulations for 90 days. As the obtained data in Figure 8A demonstrated, deformable liposomes were stable with negligible loss of entrapped drug under refrigerated condition for 90 days; while conventional liposomes showed 60% loss of drug content after 30 days and then plateaued through 90 days. The significant drug loss observed in CLP was due to the agglomeration of the vesicles, which was affected by their surface charge.

In the present study, zeta potential has been employed to estimate the surface charge. As many studies revealed,^{55–57} higher positive or negative values of zeta potential of nano vesicles indicate good physical stability due to electrostatic repulsion of individual particles. On the other hand, zeta potential value close to zero can result in particle aggregation and flocculation due to the van der Waals attractive forces.

As data summarized in Table 2 showed, zeta potential of conventional liposomes was found to be around 2 mV,

while those deformable liposomes ranged from 24–32 mV. These results confirmed with those obtained in the stability data.

The % drug lost in CLP-gel was found to be 3%, 8%, and 10% at 30, 60, and 90-day storage at room temperature, which is a significant improvement if compared to the stability data observed in the suspension. High viscosity of the hydrogel medium may be considered as a factor preventing agglomeration of the dispersed vesicles which could also contribute to higher drug stability. The deformable liposomal gel formulations were all stable for 90 days at room temperature, as displayed in Figure 8.

Conclusions

In this study, MX loaded deformable liposomal gel formulations containing transfersomes or flavosomes were prepared and tested as potential drug delivery carriers for topical use. These vesicles exhibited homogeneous particle sizes less than 120 nm with a higher entrapment rate as compared to conventional liposomes. These liposomal suspensions were then incorporated into 20% (w/w) poloxamer P407 hydrogel and characterized using rheological analysis, ex vivo permeation study through human cadaver skin and stability tests. It was shown that, despite thickening of the poloxamer 407 gel structure in comparison to the liposome-free gel, the deformable liposomal gel formulations promoted drug permeation across the skin to the deeper layers with high efficiency. The enhancement effect was also clearly visible by CLSM in comparison to the

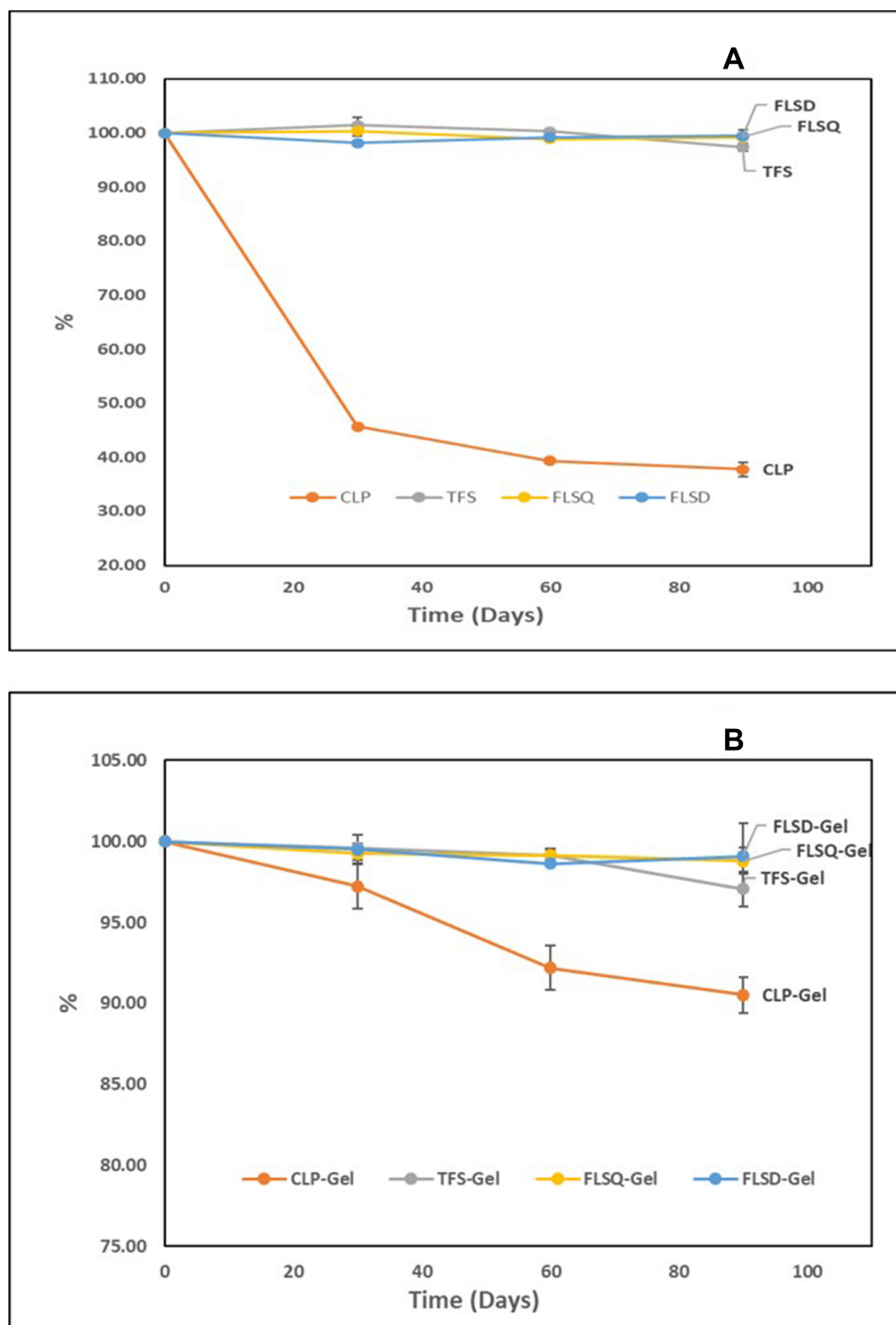


Figure 8 Stability study results of (A) meloxicam-loaded liposomal suspensions at 5±3°C for 30, 60, and 90 days, and (B) meloxicam-loaded liposomal gel formulations at 25±5°C for 30, 60, and 90 days (n=3 for each formulation).

formulation containing conventional liposomes. Notably, the flavosomal drug delivery system produced a shorter lag time compared to the transfersomal gel formulation, indicating a potential benefit for faster pain relief and anti-inflammatory effects.

Ethics Approval

As per Rutgers IRB (Institutional Review Board), our lab is exempt for ethical approval to conduct a human cadaver skin permeation study. New York Firefighters Skin Bank is an accredited AATB (American Association of Tissue

Banks) institution and is exempt as per Uniform Anatomic Gift Act. Therefore, ethical approval number is not required for this study.

Acknowledgments

The authors would like to thank BASF Corporation for providing the sample of Kolliphor® P407 (Poloxamer P407) free of charge, Lipoid LLC for providing the sample of Soybean Phosphatidylcholine free of charge, as well as Malvern Instruments for the access to the rheometer. We would like to thank Dr. Anna Froelich (Poznan University of Medical Sciences) for her valuable comments on the manuscript. This article reflects the authors' view only. Neither the Research Executive Agency nor the Polish Ministry of Science and Higher Education may be held responsible for the use which may be made of the information contained therein.

Author Contributions

Zhang Julia Zhang: Conceptualization, data curation, methodology, validation, formal analysis, investigation, visualization, writing – original draft preparation, writing – review and editing.

Tomasz Osmałek: Conceptualization, data curation, methodology, formal analysis, investigation, visualization, writing – original draft preparation, writing – review and editing.

Bozena Michniak-Kohn: Conceptualization, supervision, project administration, funding acquisition, writing – review and editing.

All authors contributed to the data analysis, drafting, or revising of the article, have agreed on the journal to which the article will be submitted, gave final approval of the version to be published, and agree to be accountable for all aspects of the work.

Funding

Part of the research was funded by the European Union's Horizon 2020 research and innovation programme under the Marie Skłodowska-Curie grant agreement No 778051 and the Ministry of Science and Higher Education of Poland fund for supporting internationally co-financed projects in 2018–2022 (agreement No 3899/H2020/2018/2). Funding for this study was provided by the Center for Dermal Research (CDR), Rutgers, The State University of New Jersey, Piscataway NJ 08854 USA.

Disclosure

The authors report no conflicts of interest in this work.

References

- Davies NM, Skjoldt NM. Clinical pharmacokinetics of meloxicam. A cyclo-oxygenase-2 preferential nonsteroidal anti-inflammatory drug. *Clin Pharmacokinet.* 1999;36(2):115–126. doi:10.2165/00003088-199936020-00003
- Pairet M, van Ryn J, Schierok H, Mauz A, Trummlitz G, Engelhardt G. Differential inhibition of cyclooxygenases-1 and -2 by meloxicam and its 4'-isomer. *Inflamm Res.* 1998;47(6):270–276. doi:10.1007/s000110050329
- Degner F, Sigmund R, Zeidler H. Efficacy and tolerability of meloxicam in an observational, controlled cohort study in patients with rheumatic disease. *Clin Ther.* 2000;22(4):400–410. doi:10.1016/S0149-2918(00)89009-8
- Deeks JJ, Smith LA, Bradley MD. Efficacy, tolerability, and upper gastrointestinal safety of celecoxib for treatment of osteoarthritis and rheumatoid arthritis: systematic review of randomised controlled trials. *BMJ.* 2002;325(7365):619. doi:10.1136/bmj.325.7365.619
- Goldman AP, Williams CS, Sheng H, et al. Meloxicam inhibits the growth of colorectal cancer cells. *Carcinogenesis.* 1998;19(12):2195–2199. doi:10.1093/carcin/19.12.2195
- Montejo C, Barcia E, Negro S, Fernandez-Carballido A. Effective antiproliferative effect of meloxicam on prostate cancer cells: development of a new controlled release system. *Int J Pharm.* 2010;387(1–2):223–229. doi:10.1016/j.ijpharm.2009.11.036
- Patel MM, Amin AF. Formulation and development of release modulated colon targeted system of meloxicam for potential application in the prophylaxis of colorectal cancer. *Drug Deliv.* 2011;18(4):281–293. doi:10.3109/10717544.2010.538447
- Arantes-Rodrigues R, Pinto-Leite R, Ferreira R, et al. Meloxicam in the treatment of in vitro and in vivo models of urinary bladder cancer. *Biomed Pharmacother.* 2013;67(4):277–284. doi:10.1016/j.biopha.2013.01.010
- Patoia L, Santucci L, Furno P, et al. A 4-week, double-blind, parallel-group study to compare the gastrointestinal effects of meloxicam 7.5 mg, meloxicam 15 mg, piroxicam 20 mg and placebo by means of faecal blood loss, endoscopy and symptom evaluation in healthy volunteers. *Br J Rheumatol.* 1996;35(Suppl 1):61–67. doi:10.1093/rheumatology/35.suppl_1.61
- Distel M, Mueller C, Bluhmki E, Fries J. Safety of meloxicam: a global analysis of clinical trials. *Br J Rheumatol.* 1996;35(Suppl 1):68–77. doi:10.1093/rheumatology/35.suppl_1.68
- Lanes SF, Rodriguez LA, Hwang E. Baseline risk of gastrointestinal disorders among new users of meloxicam, ibuprofen, diclofenac, naproxen and indomethacin. *Pharmacoepidemiol Drug Saf.* 2000;9(2):113–117. doi:10.1002/(SICI)1099-1557(200003/04)9:2<113::AID-PDS478>3.0.CO;2-2
- Wishart DSKC, Guo AC, Shrivastava S, et al. Drugbank: a comprehensive resource for in silico drug discovery and exploration. *Nucleic Acids Res.* 2006;1(34(Database issue)):D668–672. doi:10.1093/nar/gkj067
- Chen J, Gao Y. Strategies for meloxicam delivery to and across the skin: a review. *Drug Deliv.* 2016;23(8):3146–3156. doi:10.3109/10717544.2016.1157839
- Zhang J, Froelich A, Michniak-Kohn B. Topical delivery of meloxicam using liposome and microemulsion formulation approaches. *Pharmaceutics.* 2020;12(3). doi:10.3390/pharmaceutics12030282
- Zhang ZJ, Michniak-Kohn B. Flavosomes, novel deformable liposomes for the co-delivery of anti-inflammatory compounds to skin. *Int J Pharm.* 2020;585:119500. doi:10.1016/j.ijpharm.2020.119500

16. Cevc G, Blume G. New, highly efficient formulation of diclofenac for the topical, transdermal administration in ultradeformable drug carriers, Transfersomes. *Biochim Biophys Acta*. 2001;1514(2):191–205. doi:10.1016/S0005-2736(01)00369-8
17. Cevc G, Gebauer D, Stieber J, Schatzlein A, Blume G. Ultraflexible vesicles, Transfersomes, have an extremely low pore penetration resistance and transport therapeutic amounts of insulin across the intact mammalian skin. *Biochim Biophys Acta*. 1998;1368(2):201–215. doi:10.1016/S0005-2736(97)00177-6
18. Dorrani M, Garbuzenko OB, Minko T, Michniak-Kohn B. Development of edge-activated liposomes for siRNA delivery to human basal epidermis for melanoma therapy. *J Control Release*. 2016;228:150–158. doi:10.1016/j.jconrel.2016.03.010
19. El Maghraby GM, Barry BW, Williams AC. Liposomes and skin: from drug delivery to model membranes. *Eur J Pharm Sci*. 2008;34(4–5):203–222. doi:10.1016/j.ejps.2008.05.002
20. Marto J, Vitor C, Guerreiro A, et al. Ethosomes for enhanced skin delivery of griseofulvin. *Colloids Surf B Biointerfaces*. 2016;146:616–623. doi:10.1016/j.colsurfb.2016.07.021
21. Roberts MS, Mohammed Y, Pastore MN, et al. Topical and cutaneous delivery using nanosystems. *J Control Release*. 2017;247:86–105. doi:10.1016/j.jconrel.2016.12.022
22. Mayba JN, Gooderham MJA. Guide to topical vehicle formulations. *J Cutan Med Surg*. 2018;22(2):207–212. doi:10.1177/1203475417743234
23. Buwalda SJ, Boere KW, Dijkstra PJ, Feijen J, Vermonden T, Hennink WE. Hydrogels in a historical perspective: from simple networks to smart materials. *J Control Release*. 2014;190:254–273. doi:10.1016/j.jconrel.2014.03.052
24. Jung YS, Park W, Park H, Lee DK, Na K. Thermo-sensitive injectable hydrogel based on the physical mixing of hyaluronic acid and Pluronic F-127 for sustained NSAID delivery. *Carbohydr Polym*. 2017;156:403–408. doi:10.1016/j.carbpol.2016.08.068
25. Dumortier G, Grossiord JL, Agnely F, Chaumeil JC. A review of poloxamer 407 pharmaceutical and pharmacological characteristics. *Pharm Res*. 2006;23(12):2709–2728. doi:10.1007/s11095-006-9104-4
26. Ban E, Park M, Jeong S, et al. Poloxamer-based thermoreversible gel for topical delivery of emodin: influence of p407 and p188 on solubility of emodin and its application in cellular activity screening. *Molecules*. 2017;22(2):246. doi:10.3390/molecules22020246
27. Akbarzadeh A, Rezaei-Sadabady R, Davaran S, et al. Liposome: classification, preparation, and applications. *Nanoscale Res Lett*. 2013;8(1):102. doi:10.1186/1556-276X-8-102
28. Duangjit S, Obata Y, Sano H, et al. Comparative study of novel ultradeformable liposomes: mentosomes, transfersomes and liposomes for enhancing skin permeation of meloxicam. *Biol Pharm Bull*. 2014;37(2):239–247. doi:10.1248/bpb.b13-00576
29. Xu X, Khan MA, Burgess DJ. A quality by design (QbD) case study on liposomes containing hydrophilic API: II. Screening of critical variables, and establishment of design space at laboratory scale. *Int J Pharm*. 2012;423(2):543–553. doi:10.1016/j.ijpharm.2011.11.036
30. Garg V, Singh H, Bhatia A, et al. Systematic development of trans-ethosomal gel system of piroxicam: formulation optimization, in vitro evaluation, and ex vivo assessment. *AAPS PharmSciTech*. 2017;18(1):58–71. doi:10.1208/s12249-016-0489-z
31. Zeb A, Qureshi OS, Kim HS, Cha JH, Kim HS, Kim JK. Improved skin permeation of methotrexate via nanosized ultradeformable liposomes. *Int J Nanomedicine*. 2016;11:3813–3824. doi:10.2147/IJN.S109565
32. Lin H, Xie Q, Huang X, et al. Increased skin permeation efficiency of imperatorin via charged ultradeformable lipid vesicles for transdermal delivery. *Int J Nanomedicine*. 2018;13:831–842. doi:10.2147/IJN.S150086
33. Tavano L, Muzzalupo R, Cassano R, Trombino S, Ferrarelli T, Picci N. New sucrose cocoate based vesicles: preparation, characterization and skin permeation studies. *Colloids Surf B Biointerfaces*. 2010;75(1):319–322. doi:10.1016/j.colsurfb.2009.09.003
34. Bozzuto G, Molinari A. Liposomes as nanomedical devices. *Int J Nanomedicine*. 2015;10:975–999. doi:10.2147/IJN.S68861
35. Taladrid D, Marin D, Aleman A, Alvarez-Acero I, Montero P, Gomez-Guillen MC. Effect of chemical composition and sonication procedure on properties of food-grade soy lecithin liposomes with added glycerol. *Food Res Int*. 2017;100(Pt1):541–550. doi:10.1016/j.foodres.2017.07.052
36. Lopez-Pinto JM, Gonzalez-Rodriguez ML, Rabasco AM. Effect of cholesterol and ethanol on dermal delivery from DPPC liposomes. *Int J Pharm*. 2005;298(1):1–12. doi:10.1016/j.ijpharm.2005.02.021
37. Duangjit S, Opanasopit P, Rojanarata T, Ngawhirunpat T. Characterization and in vitro skin permeation of meloxicam-loaded liposomes versus transfersomes. *J Drug Deliv*. 2011;2011:418316. doi:10.1155/2011/418316
38. Gupta PN, Mishra V, Rawat A, et al. Non-invasive vaccine delivery in transfersomes, niosomes and liposomes: a comparative study. *Int J Pharm*. 2005;293(1–2):73–82. doi:10.1016/j.ijpharm.2004.12.022
39. Bragagni M, Mennini N, Maestrelli F, Cirri M, Mura P. Comparative study of liposomes, transfersomes and ethosomes as carriers for improving topical delivery of celecoxib. *Drug Deliv*. 2012;19(7):354–361. doi:10.3109/10717544.2012.724472
40. Hua S. Lipid-based nano-delivery systems for skin delivery of drugs and bioactives. *Front Pharmacol*. 2015;6:219.
41. Buhse L, Kolinski R, Westenberger B, et al. Topical drug classification. *Int J Pharm*. 2005;295(1–2):101–112. doi:10.1016/j.ijpharm.2005.01.032
42. Li J, Mooney DJ. Designing hydrogels for controlled drug delivery. *Nat Rev Mater*. 2016;1:12.
43. Yu T, Malcolm K, Woolfson D, Jones DS, Andrews GP. Vaginal gel drug delivery systems: understanding rheological characteristics and performance. *Expert Opin Drug Deliv*. 2011;8(10):1309–1322. doi:10.1517/17425247.2011.600119
44. As R, Sirivat A, Vayumhasuwan P. Viscoelastic properties of Carbopol 940 gels and their relationships to piroxicam diffusion coefficients in gel bases. *Pharm Res*. 2005;22(12):2134–2140. doi:10.1007/s11095-005-8244-2
45. Fakhari A, Corcoran M, Schwarz A. Thermogelling properties of purified poloxamer 407. *Heliyon*. 2017;3(8):e00390. doi:10.1016/j.heliyon.2017.e00390
46. Pandita D, Ahuja A, Lather V, et al. Development of lipid-based nanoparticles for enhancing the oral bioavailability of paclitaxel. *AAPS PharmSciTech*. 2011;12(2):712–722. doi:10.1208/s12249-011-9636-8
47. Instruments M. DLS Technical Note. MRK656-01. Available from: https://warwick.ac.uk/fac/cross_fac/sciencecity/programmes/internal/themes/am2/booking/particlesize/intro_to_dls.pdf. Accessed November 16, 2020.
48. Liu D, Hu H, Lin Z, et al. Quercetin deformable liposome: preparation and efficacy against ultraviolet B induced skin damages in vitro and in vivo. *J Photochem Photobiol B*. 2013;127:8–17. doi:10.1016/j.jphotobiol.2013.07.014
49. Kirjavainen M, Urtti A, Valjakka-Koskela R, Kiesvaara J, Monkkonen J. Liposome-skin interactions and their effects on the skin permeation of drugs. *Eur J Pharm Sci*. 1999;7(4):279–286. doi:10.1016/S0928-0987(98)00037-2
50. Pawlikowska-Pawlega B, Gruszecki WI, Misiak L, et al. Modification of membranes by quercetin, a naturally occurring flavonoid, via its incorporation in the polar head group. *Biochim Biophys Acta*. 2007;1768(9):2195–2204. doi:10.1016/j.bbamem.2007.05.027

51. Hendrich AB, Malon R, Pola A, Shirataki Y, Motohashi N, Michalak K. Differential interaction of Sophora isoflavonoids with lipid bilayers. *Eur J Pharm Sci.* 2002;16(3):201–208. doi:10.1016/S0928-0987(02)00106-9
52. Kim YA, Tarahovsky YS, Yagolnik EA, Kuznetsova SM, Muzafarov EN. Lipophilicity of flavonoid complexes with iron (II) and their interaction with liposomes. *Biochem Biophys Res Commun.* 2013;431(4):680–685. doi:10.1016/j.bbrc.2013.01.060
53. Movileanu L, Neagoe I, Flonta ML. Interaction of the antioxidant flavonoid quercetin with planar lipid bilayers. *Int J Pharm.* 2000;205(1–2):135–146. doi:10.1016/S0378-5173(00)00503-2
54. Saija A, Scalese M, Lanza M, Marzullo D, Bonina F, Castelli F. Flavonoids as antioxidant agents: importance of their interaction with biomembranes. *Free Radic Biol Med.* 1995;19(4):481–486. doi:10.1016/0891-5849(94)00240-K
55. Agarwal S, Murthy RSR, Harikumar SL, Garg R. Quality by design approach for development and characterisation of solid lipid nanoparticles of quetiapine fumarate. *Curr Comput Aided Drug Des.* 2020;16(1):73–91. doi:10.2174/1573409915666190722122827
56. Kedar U, Phutane P, Shidhaye S, Kadam V. Advances in polymeric micelles for drug delivery and tumor targeting. *Nanomedicine.* 2010;6(6):714–729. doi:10.1016/j.nano.2010.05.005
57. Beck-Broichsitter M, Ruppert C, Schmehl T, et al. Biophysical investigation of pulmonary surfactant surface properties upon contact with polymeric nanoparticles in vitro. *Nanomedicine.* 2011;7(3):341–350. doi:10.1016/j.nano.2010.10.007

International Journal of Nanomedicine

Dovepress

Publish your work in this journal

The International Journal of Nanomedicine is an international, peer-reviewed journal focusing on the application of nanotechnology in diagnostics, therapeutics, and drug delivery systems throughout the biomedical field. This journal is indexed on PubMed Central, MedLine, CAS, SciSearch®, Current Contents®/Clinical Medicine,

Journal Citation Reports/Science Edition, EMBase, Scopus and the Elsevier Bibliographic databases. The manuscript management system is completely online and includes a very quick and fair peer-review system, which is all easy to use. Visit <http://www.dovepress.com/testimonials.php> to read real quotes from published authors.

Submit your manuscript here: <https://www.dovepress.com/international-journal-of-nanomedicine-journal>